Local Chain Segregation and Entanglements in a Confined Polymer Melt

Nam-Kyung Lee,[1,2] Diddo Diddens,[2] Hendrik Meyer,[2] and Albert Johner[1,2]
[1]Institute of Fundamental Physics, Department of Physics, Sejong University, Seoul 05006, Korea
[2]Institut Charles Sadron, Université de Strasbourg, CNRS UPR22, 23 rue du Loess 67034, Strasbourg cedex 2, France
(Received 29 January 2016; revised manuscript received 16 December 2016; published 8 February 2017)

The reptation mechanism, introduced by de Gennes and Edwards, where a polymer diffuses along a fluffy tube, defined by the constraints imposed by its surroundings, convincingly describes the relaxation of long polymers in concentrated solutions and melts. We propose that the scale for the tube diameter is set by local chain segregation, which we study analytically. We show that the concept of local segregation is especially operational for confined geometries, where segregation extends over mesoscopic domains, drastically reducing binary contacts, and provide an estimate of the entanglement length. Our predictions are quantitatively supported by extensive molecular dynamics simulations on systems consisting of long, entangled chains.

DOI: 10.1103/PhysRevLett.118.067802

The celebrated reptation model, introduced by de Gennes and Edwards, provides relatively simple insight into the dynamics of long polymers in a concentrated solution or melt [1–3]. The central idea is that the everpresent noncrossing constraint allows chains to slide by each other, but not to pass through. In this picture, one tagged chain in the system moves under the constraints imposed by the surrounding chains, which build "topological" obstacles called entanglements (Fig. 1). An important parameter of the model is the diameter r_t of the reptation tube or the associated average chemical distance (number of monomers) between entanglements along a chain $N_e = (r_t/b)^2$, with b the monomer size. The tube diameter is a material parameter linked to the plateau modulus $G = k_bT/r_t^3$, which, together with the local friction coefficient, describes many of the unique rheological properties of entangled melts [4]. In practice, r_t is between 3 and 10 nm for flexible polymers [3].

The heuristic Lin-Noolandi ansatz defines the tube diameter as the scale for which a given chain shares space with a prescribed number ν of other chains (≈ 20 for all flexible polymers [5]) [3,6,7]. This defines the length $r_t = \nu/(cb^2)$, which is a decreasing function of the monomer concentration c. The "packing length" r_p [8], introduced as $r_p = 1/(cb^2)$, is hence expected to be the natural scale of the problem. A compilation of numerical and some experimental data by Everaers [9] also supports the idea that the packing length and the tube diameter gained from the plateau modulus are proportional to each other. It is inferred that r_p contains all the information about microscopic details. Beyond, chains wrap in a universal way. The large prefactor between r_t and r_p is somewhat puzzling. Recently, it was shown that entanglements are essentially binary [10–12] and further suggested [13] that a section of length N_e builds up half of the concentration at its center of mass. This specific argument leads to [14] $r_t = 8(9/2\pi)^{3/2} r_p \approx 14 r_p$. A different dynamical approach to the tube by Sussman [15] leads to a similar estimate. Two recent studies ([12,16]) show that the dynamical approach of the tube initiated by Likhtman [17] is compatible with the approach by Everaers [9] (or Kröger [18] and Theodorou [19]) and a knot-distribution entropy-based definition by Qin and Milner [12]. Generalizing the concept of packing length to confined geometries is not straight forward. Instead, we consider local segregation between chains analytically. Both concepts are essentially equivalent in the bulk, but segregation is even enhanced in confined systems. Disentanglement upon confinement was reported from both simulation and experiment [20,21]. We will focus on confinement in a slit of width h. Local chain segregation turns out to extend over mesoscopic (lateral) distances, which ultimately penalizes binary contacts (*a fortiori* suppressing complex knots) and has a strong impact on mutual entanglements, which was overlooked so far. Bringing a monomer of a foreign chain close to a monomer of a given chain costs some free energy related to the so-called correlation-hole effect [2]. Below, energies are expressed in thermal units k_BT.

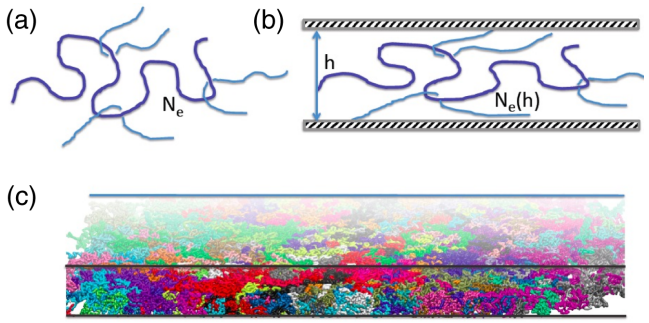

FIG. 1. Systems of polymer entanglements (a) in a bulk (b) in a slit of width h. A labeled test chain (bold) and entangled similar chains (thin) are shown. (c) An image of a confined polymer melt obtained from a MD simulation of chain length $N = 1024$, with slit width $h = 9\sigma_0$. (See simulation description.)

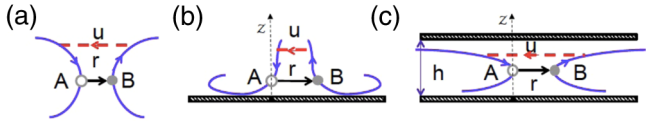

FIG. 2. Integrated interaction U between chains when a separation $\mathbf{r}$ is imposed between a monomer A of one chain and a monomer B of the other chain in various geometries: (a) bulk, (b) a half-space with von Neumann boundary conditions, (c) a slit of width h where A and B are located at $z = h/2$. Momentum q is circulating in the upper loop: each polymer line (solid blue) carries a factor $1/(q^2a^2)$; a red dashed line carries an interaction u. This leads to the Coulombic $\tilde{U}(q)$ in Eq. (1). More details are given in the Supplemental Material [23].

Let us first show this point on the simple case of a free (unconfined) system Fig. 2(a). For a melt of long chains in the incompressible limit, the interaction between monomers a distance $r > b$ apart is given by $u(q) = (q^2a_D^2)/(2c)$ in momentum space with $\mathbf{q}$, Fourier conjugate of $\mathbf{r}$, and $a_D^2 = b^2/(2D)$ a monomeric length, D being the dimension of space [22] (also see Fig. 1(a) in Supplemental Material [23]). It is then easy to show that for two infinite chains, say black and white, the corresponding (integrated) interaction $U(r)$ when a distance r is imposed between a black and a white monomer is Coulombic to lowest order in all dimensions (see Fig. 1(b) in Supplemental Material [23]):

$$\tilde{U}(q) = \frac{2k_BT}{q^2a_D^2c}, \qquad U(r) = \frac{k_BT}{2\pi a^2cr} \quad \text{for } D = 3, \tag{1}$$

where $a = a_3$. Finite size effects are not so essential in 3D free space, but will turn out important in subsequent cases. Here and below, we only consider the integrated interaction between midpoints. The real space potential [Eq. (1)] is multiplied by the cutoff function:

$$f_{\text{cut}}(r) = 2\text{erfc}\left(\frac{r}{\sqrt{2}R_g}\right) - \text{erfc}\left(\frac{r}{2R_g}\right), \tag{2}$$

with $R_g = \sqrt{Na^2}$ as a cutoff length. The cutoff entails a shallow minimum at $r \approx 1.9R_g$, which might induce a very weak "colloidal" organization of the middle monomers of the chains. The foreign monomers (say white) typically approach a given monomer of a labeled chain (say black) down to distance r where U reaches the thermal energy k_BT. At shorter distances, a monomer of a given chain is merely surrounded by monomers of the same chain. This criterion defines the scale of "segregation length" as below:

$$r_s = \frac{1}{2\pi a^2c}. \tag{3}$$

Strictly speaking, Eq. (1) is accurate for $r \gtrsim r_s$, where the interaction does not exceed k_BT. At this stage, our approach is nothing but an alternative, admittedly more complicated, way to obtain the length scale r_p (together with the distribution of foreign monomers).

Because the Coulomb interaction is longer ranged at lower dimensions, we expect segregation to be enhanced by confinement. In the general case of a cavity, the Laplace operator $-a^2\Delta$ admits eigenvalues ϵ_n and eigenfunctions ψ_n, defined for the generic reflecting (von Neumann) boundary conditions [24]. In lower dimensions, Coulombic interactions are sensitive to the system size and we keep track of the finite chain size N. For simplicity, we fix the two chain midpoints at $\mathbf{r}_A$ and $\mathbf{r}_B$ and calculate the interaction including the uniform ground state with $\epsilon_0 = 0$:

$$U(\mathbf{r}_A, \mathbf{r}_B) = \sum_k 2\frac{(1 - e^{-\epsilon_k N/2})^2}{c\epsilon_k}\psi_k(\mathbf{r}_A)\psi_k(\mathbf{r}_B), \tag{4}$$

where the eigenfunctions are normalized to the volume of the cavity. In free space, the ψ_k are plane waves, and we recover the previously used residual interaction. For infinite chains, the interaction given by Eq. (4) is proportional to the Green function for electrostatics with reflecting boundaries, and the electrostatic analogy formally holds.

Let us now consider two chains (A) and (B) in a melt of similar chains filling the half space $z > 0$ [Fig. 2(b)]. The positions of the constrained monomers are designated by $\mathbf{r_A}\{z_A, \rho_A = 0\}$ and $\mathbf{r_B}\{z_B, \rho_B = \rho\}$ in cylindrical coordinates. By analogy with electrostatics, and accounting for the *image charge* of the same sign, we write the integrated interaction:

$$U_{1/2}(\rho, z_A, z_B) = U\left(\sqrt{\rho^2 + z_-^2}\right) + U\left(\sqrt{\rho^2 + z_+^2}\right), \tag{5}$$

where $z_- = z_A - z_B$ and $z_+ = z_A + z_B$. For finite chains, each of the U functions in Eq. (5) comes with the cutoff function, Eq. (2). Equation (5) merges with the interaction in the bulk at large distances from the wall. Very close to the wall ($z_A = 0$), the exclusion zone defined from Eq. (5) by $U_{1/2} = k_BT$ is a half sphere of radius $2r_s$. (See also Fig. 2 in Supplemental Material [23].) Away from the wall, the exclusion zone elongates perpendicular to the wall and detaches from the wall for $z_A = 2r_s$. The bulk exclusion zone is recovered at $z_A \approx 5r_s$. It is natural to characterize the exclusion zone by the area of its generating section, which becomes πr_s^2 in the bulk and is doubled at the wall. These results are qualitatively equivalent to earlier findings by Brown [25], using the qualitative packing argument and more recently, by Qin [26]. Equation (5) can be also recovered as a limiting case of confinement in a slit discussed below.

For a slit of width h [Fig. 2(c)], the two in-plane directions are invariant by translation and $\epsilon_k = q_\parallel^2a^2 + \pi^2n^2a^2/h^2$, where n runs over the natural numbers, including zero. After taking the Laplace transform with respect to N, the series in Eq. (4) can be summed up as:

$$U_{\rm slit} = \frac{1}{pca^2}\{2f(2p/a^2) - f(p/a^2)\}, \quad (6)$$

with $f(x) = f_+(x) + f_-(x)$ and

$$f_\pm(x) = \frac{\cosh\left[(q_\parallel^2 + x)^{1/2}(h - |z_\pm|)\right]}{(q_\parallel^2 + x)^{1/2}\sinh[(q_\parallel^2 + x)^{1/2}h]},$$

where p is the Laplace conjugate of N. The interaction Eq. (6), calculated in the middle of the slit, (see Fig. 1(d) in Supplemental Material [23]), exhibits several regimes summarized in Fig. 3. The interaction between midmonomers of two chains embedded in a melt of similar chains is essentially Coulombic. Close to a wall, we must account for the image charge of the same sign. In a slit of width h, the interaction is 3D at distances shorter than $h/\log(R_g/h)$ and 2D at distances larger than h. As long as r_s belongs to the 3D regime, Eq. (3) holds. Finite chain length entails screening of the interaction beyond a distance R_g. At intermediate distances between h and R_g, R_g defines the cutoff length of the logarithmic interaction. We shall consider 2D coarse-grained (CG) chains comprising CG monomers of diameter h and monomer content h^2/b^2.

At distances larger than h, the system merely behaves as 2D polymers with crossings [22,27]. Beyond perturbation, the crossing probabilities are given by the vertex exponents $\sigma_f = f(2-f)/4$, with $f(\geq 1)$ the order of the vertex [22,27]. The partition function of a network factorizes in vertex and loop contributions [28]. For a network composed of strands of size n, each vertex contributes a factor $(1 + \kappa \log n)^{\sigma_f}$ to the partition function, with $\kappa = r_s/(2h)$ the Ginzburg parameter, which characterizes tube confinement, and each (independent) loop contributes a factor b^2/R_e^2, with $R_e^2 = nb^2(1 + \kappa \log n)$ [29]. For example, the partition function of a simple cross between two 2D chains of length n is $Z_4 \sim \{1 + [r_s/(2h)]\log n\}^{-2}$. To make connection with Fig. 3, we can express the fraction of foreign (coarse-grained) monomers at a distance ρ from a given (coarse-grained) monomer [22,27]

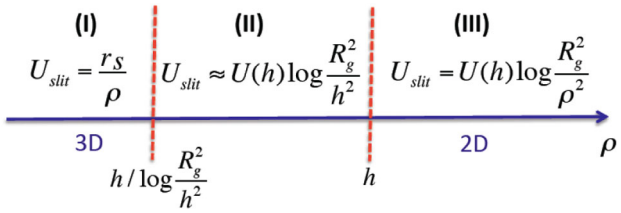

FIG. 3. Interaction $U_{\rm slit}$ in the midplane of the slit as a function of the lateral distance ρ: crossover from the 3D regime to the 2D regime with $U(h) = r_s/h$. The interaction is nearly constant in regime (II). The cutoff beyond R_g is discussed in the Supplemental Material [23].

$$P(\rho) = \left(\frac{1 + \frac{r_s}{2h}\log(\rho^2/h^2)}{1 + \frac{r_s}{2h}\log(Nb^2/h^2)}\right)^2. \quad (7)$$

This generally applies and matches the perturbative 2D expression of $U_{\rm slit}$ (Fig. 3).

As long as $h \gg r_s \log(Nb^2/h^2)$, the CG monomers freely mix and the 3D situation holds, up to single wall effects [25]. Beyond perturbation, contacts between CG chains are strongly reduced, although CG monomers of extension h strongly overlap for $h > r_s$. Each CG monomer lives in a 3D environment and experiences binary entanglements with overlapping CG monomers. As a result, the number of mutual entanglements is proportional to the fraction $\mathrm{P}(h)$ of mutual contacts (contacts with foreign chains). Confinement hence reduces the number of mutual entanglements by a factor $\mathrm{P}(h)$. Accordingly:

$$N_e(h) \approx N_e\left(1 + \frac{r_s \log(Nb^2/h^2)}{2h}\right)^2. \quad (8)$$

The 3D regime (and 3D type entanglements) are lost for $h < r_s$. This ultraconfined regime may only be relevant to concentrated solutions where r_s is larger than in the strict melt. Now, a sharp cut border between segregation and mixing is somewhat arbitrary. Seeking for the distance ρ, where the probability to find a foreign monomer is P, we obtain:

$$\frac{\rho}{h} = e^{-h(1-\sqrt{\mathrm{P}})/(2r_s)}\left(\frac{Nb^2}{h^2}\right)^{\frac{\sqrt{\mathrm{P}}}{2}}. \quad (9)$$

We may choose $\mathrm{P} = 1/e$ as the value at the border, which corresponds to our previous criterion $U = k_BT$. For strong confinement $h < r_s$, a given chain expels foreign monomers out of a ribbon of width $\rho \sim (Na^2/h^2)^{(1/2\sqrt{e})}h$ increasing with chain length. For $h > r_s$, the width of the ribbon strongly decreases with h and qualitatively matches h for the gap width $h \sim r_s \log N$.

Even when a given polymer is softly confined to an ill-defined ribbon [Eq. (9)], it still can hook with other chains, forming scarce entanglements involving (at least) coarse-grained double contacts. More complex entanglements (or knots) involving higher order vertices are scarcer. At any time, constraints are materialized by tight hooks (see Fig. 4). It is assumed that their average number can be obtained from the ensemble average. Their abundance is quantified by the hook partition function given in Eq. (10) below. The derivation of the hook partition function Z_h [Eq. (10)] step by step, starting from simpler hooks, is detailed in the Supplemental Material [23]. It is convenient to work with reduced chemical distances $\tilde{n} = nb^2/h^2$, counted in units of blobs. We will restore natural units in the final discussion. After integration of the partition function Z (see Table in Supplemental Material [23]) over

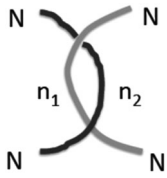

FIG. 4. Statistical weight of a hook between two chains in a slit (2D regime), $n_1 < n_2 < N$. The partition function Z_h of a hook between two chains is obtained step by step from that of simpler hooks (see Supplemental Material [23]).

$\tilde{n}_1$ from 0 to $\tilde{n}_2$, the partition function of a single hook of size $n \sim n_2$ between two chains is given by:

$$Z_h \sim \left(1 + \frac{r_s}{2h}\log\frac{Nb^2}{h^2}\right)^{-2}\left(1 + \frac{r_s}{2h}\log\frac{nb^2}{h^2}\right)^{-3}, \quad (10)$$

where $\sigma_4 = -2$ has been inserted. As discussed above, the hook should be tight and $\tilde{n}$ remain almost of order unity. For strong polymer confinement $r_s > h$, where CG monomers do not typically overlap, the partition function Z_h allows us to directly assess the average distance between hooks along a given chain $N_h(h) \sim (h^2/b^2)/Z_h$,

$$N_e(h) \sim \frac{r_s^5}{b^2h^3}[\log(Nb^2/h^2)]^2; \quad (r_s > h). \quad (11)$$

To test our main prediction, Eq. (8), large scale MD simulations were set up using the same bead-spring model as in Refs. [20,32]. The MD has been combined with a double-bridging algorithm [33–35] to accelerate decorrelation of configurations for the sampling of static properties. Only the use of the double-bridging moves made it possible to obtain reliable statistics up to chain length $N = 2048$. The simulation box comprises at least 96 chains. The gap width ranges from twice the radius of gyration R_g to about 4 monolayers thick. Below, we focus on the confined regime $h < R_g$. In the simulation, R_g amounts to $\approx 17.5\sigma_0$ for $N = 1024$ and $\approx 24.5\sigma_0$ for $N = 2048$, with σ_0 the bead diameter. We present only data for $N = 1024$ and $N = 2048$, which still exhibit a few entanglements in the thinnest film. To reveal the mutual entanglements, we adapted the stretching procedure [9], introduced by Everaers. From the analysis of the entanglement network, we obtain the entanglement lengths $N_e(h)$ for the various gap widths, h. $N_e(h)$ is preaveraged over a group of twelve configurations for each h. The results of the (typically 3) determinations were further averaged and the dispersion among different determinations is displayed as precision in data shown in Fig. 5. The standard bulk value of the entanglement length N_e was measured separately; the stretching procedure delivers a value slightly increasing, with chain length designated as N_e^{bk} below.

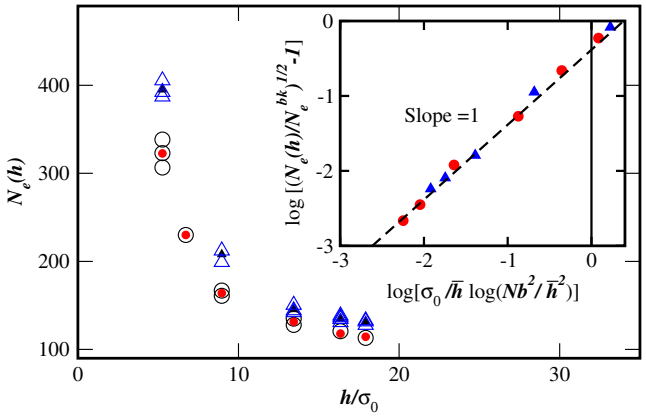

FIG. 5. Measured value of $N_e(h)$ from MD simulation of long polymer chains ($\triangle$ $N = 1024$, $\circ$ $N = 2048$) in gaps of various width h. Empty symbols are independent realization and solid symbols represent the averaged value for each h. In the inset, $\sqrt{N_e(h)/N_e^{bk}} - 1$ versus $(\sigma_0/\bar{h})\log(Nb^2/\bar{h}^2)$ is plotted in log scales. The size of the symbols (≈ 0.1) reflects the precision of the data ($\approx 10\%$).

The obtained values of $N_e(h)$ are plotted against h in Fig. 5, which clearly shows an increase of $N_e(h)$ upon confinement. Note that previously published simulation studies have been limited to weakly entangled ($N = 256$) bulk chains [20] and accordingly, reported complete disentanglement upon strong confinement. In contrast, we observe gradual disentanglement: the gap width decreases by a factor 5 and the entanglement length is tripled. To make direct connection with Eq. (8), we present scaled data in the inset of Fig. 5, as was done for the in-plane radius of gyration squared in Ref. [31]. In the scaling plot, we show log-log plot of $(\sqrt{N_e(h,N)/N_e^{bk}(N)} - 1)$ versus the coupling $(\sigma_0/\bar{h})\log(Nb^2/\bar{h}^2)$. The gap thickness $\bar{h}$, smaller than h by $1.08\sigma_0$, accounts for depletion effects as discussed in Supplemental Material [23]. Adjusting the strength of the coupling amounts to a vertical shift in this representation. The data for both chain lengths $N = 1024$ and $N = 2048$ collapse on a straight line parallel to the bisector, which is consistent with the prediction Eq. (8). The retained value of the y intercept -0.40 corresponds to the coupling strength $e^{-0.40} \approx 0.67$, which is somewhat larger than the estimate from the Edwards model (see Eq. (3) and Supplemental Material [23]), $r_s/(2\sigma_0) \approx 0.45$ for the raw simulation parameters ($c = 0.68\sigma_0^{-3}$, $b^2 = 1.8\sigma_0^2$). The current plot covers about one decade in the scaling variable, which is sufficient to confirm the slope 1.

We focused on interchain entanglements, which are most relevant to rheological types of experiments (see Ref. [36]). We predict a drastic reduction of mutual entanglements upon confinement. This can be formally understood as being on the way to strict 2D where there are no entanglements at all and chains are completely segregated (with a fractal border) [22]. Our prediction is quantitatively

supported by extensive MD simulation for the system of long entangled polymer chains ($N = 1024$ and 2048). Currently available experiments on free standing films do not explore films much thinner than the radius of gyration in the bulk [36].

Our work is in part supported by National Research Foundation grants provided by Korean government (NRF-2014R1A1A2055681 and NRF-2016R1D1A1B03931049). We thank the HPC center of Université de Strasbourg for a generous grant of CPU time through the programme Equip@MESO.

[1] M. Doi and S. F. Edwards, *The Theory of Polymer Dynamics* (Oxford University Press, New York, 1988).
[2] P. G. de Gennes, *Scaling Concepts in Polymer Physics* (Cornell University Press, Ithaca, 1980).
[3] M. Rubinstein and R. H. Colby, *Polymer Physics* (OUP, Oxford, 2003).
[4] T. C. B McLeish, Adv. Phys. **51**, 1379 (2002).
[5] L. J. Fetters, D. J. Lohse, D. Richter, T. A. Witten, and A. Zirkel, Macromolecules **27**, 4639 (1994).
[6] Y. H. Lin, Macromolecules **20**, 3080 (1987).
[7] T. A. Kavassalis and J. Noolandi, Phys. Rev. Lett. **59**, 2674 (1987).
[8] T. A. Witten, S. T. Milner, and Z. G. Wang, in *Multiphase Macromolecular Systems*, edited by B. M. Culbertson (Plenum Press, New York, 1989).
[9] R. Everaers, S. K. Sukumaran, G. S. Grest, C. Svaneborg, A. Sivasubramanian, and K. Kremer, Science **303**, 823 (2004).
[10] R. Everaers, Phys. Rev. E **86**, 022801 (2012).
[11] N. Uchidaa, G. S. Grest, and R. Everaers, J. Chem. Phys. **128**, 044902 (2008).
[12] J. Qin and S. T. Milner, Macromolecules **47**, 6077 (2014).
[13] A. Rosa and R. Everaers, Phys. Rev. Lett. **112**, 118302 (2014).
[14] H. Yamakawa, *Modern Theory of Polymer Solutions* (Harper & Row, New York, 1972).
[15] D. M. Sussman and K. S. Schweizer, Phys. Rev. Lett. **109**, 168306 (2012).
[16] T. Ge, S. Panyukov, and M. R. Rubinstein, Macromolecules **49**, 708 (2016).
[17] D. J. Read, K. Jagannathan, and A. E. Likhtman, Macromolecules **41**, 6843 (2008).
[18] M. Kröger, Comput. Phys. Commun. **168**, 209 (2005).
[19] C. Tzoumanekas and D. N. Theodorou, Macromolecules **39**, 4592 (2006).
[20] H. Meyer, T. Kreer, A. Cavallo, J. P. Wittmer, and J. Baschnagel, Eur. Phys. J. Spec. Top. **141**, 167 (2007).
[21] D. M. Sussman, W. S. Tung, K. I. Winey, K. Schweizer, and R. A. Riggleman, Macromolecules **47**, 6462 (2014).
[22] A. Semenov and A. Johner, Eur. Phys. J. E **12**, 469 (2003).
[23] See Supplemental Material at http://link.aps.org/supplemental/10.1103/PhysRevLett.118.067802 for calculations of interactions in confined geometries, derivations of partition functions and simulation descriptions.
[24] N.-K. Lee, J. Farago, H. Meyer, J. P. Wittmer, J. Baschnagel, S. Obukhov, and A. Johner, EPL **93**, 48002 (2011).
[25] H. R. Brown and T. Russel, Macromolecules **29**, 798 (1996).
[26] W. Bisbee, J. Qin, and S. T. Milner, Macromolecules **44**, 8972 (2011).
[27] A. Johner, F. Thalmann, J. Baschnagel, H. Meyer, S. Obukhov, and J. P. Wittmer, J. Stat. Mech. (2014) P04024.
[28] B. Duplantier, J. Stat. Phys. **54**, 581 (1989).
[29] Earlier MD simulation studies of shorter ($N = 256$ [30] and $N = 512$ [31]), not too dense polymers, provided evidence for logarithmic renormalization factors (for R_g^2) over some range.
[30] A. Cavallo, M. Müller, J. P. Wittmer, A. Johner, and K. Binder, J. Phys: Condens. Matter **17**, 1697 (2005).
[31] A. Galuschko, M. Lang, T. Kreer, and J. U. Sommer, Soft Mater. **12**, S49 (2014).
[32] H. Meyer, J. P. Wittmer, T. Kreer, P. Beckrich, A. Johner, J. Farago, and J. Baschnagel, Eur. Phys. J. E **26**, 25 (2008).
[33] J. P. Wittmer, P. Beckrich, H. Meyer, A. Cavallo, A. Johner, and J. Baschnagel, Phys. Rev. E **76**, 011803 (2007).
[34] J. Baschnagel, J. P. Wittmer, and H. Meyer, *Computational Soft Matter: From Synthetic Polymers to Proteins*, edited by N. Attig, K. Binder, H. Grubmüller, and K. Kremer (NIC Series, Jülich, 2004), Vol. 23, pp. 83–140.
[35] R. Auhl, R. Everaers, G. S. Grest, K. Kremer, and S. J. Plimpton, J. Chem. Phys. **119**, 12718 (2003).
[36] L. Si, M. V. Massa, K. Dalnoki-Veress, H. R. Brown, and R. A. L. Jones, Phys. Rev. Lett. **94**, 127801 (2005).